Forensic Science International 362 (2024) 112172

Contents lists available at ScienceDirect

Forensic Science International

journal homepage: www.elsevier.com/locate/forsciint

Preliminary investigations into the use of the ancient pigments Han blue and Han purple as luminescent dusting powders for the detection of latent fingermarks

Ruby La Rocca [a], Rebecca Pitman [a], Sorour Shahbazi [a], Thais Lópes [a], Elena Dallerba [a], Massimiliano Massi [a], Gregory D. Smith [b], Simon W. Lewis [a,*]

[a] School of Molecular and Life Sciences, Curtin University, GPO Box U1987, Perth, Western Australia 6845, Australia
[b] Conservation Science Department, Indianapolis Museum of Art at Newfields, 4000 Michigan Road, Indianapolis, IN 46208-3326, USA

ARTICLE INFO

Keywords:
Latent fingermark detection
Fingerprint dusting powders
Near-infrared luminescence
Artists pigments
Sustainable development

ABSTRACT

Here we present our preliminary studies into the inorganic pigments Han blue ($BaCuSi_4O_{10}$) and Han purple ($BaCuSi_2O_6$) as near-infrared luminescent fingerprint dusting powders. These pigments were developed in ancient China around 800 BCE and both show luminescence in the NIR region. There remains, however, ambiguity in the literature concerning their photophysical properties. Samples of Han blue and Han purple artist's pigments were characterized by optical microscopy, infrared, ultraviolet-visible absorbance and luminescence spectroscopy. Their performance as fingerprint dusting powders, without any further treatment, on non-porous surfaces were compared to exfoliated lipophilic coated Egyptian blue and commercial fluorescent powders in a pilot study. These results demonstrate for the first time that both ancient pigments show promise as alternative dusting powders for latent fingermarks.

1. Introduction

Dusting powders are widely used as the main development method for latent fingermarks deposited on non-porous surfaces [1–3]. They offer a cost-effective development technique, that is ideal for non-porous surfaces [3–5]. The dusting technique offers versatility in colour and application method, with minimal destruction to the evidence, as often experienced with chemical development techniques [1]. However, a key challenge that remains is the visualisation of developed fingermarks, on patterned, multicoloured, or reflective surfaces [3].

The use of luminescent dusting powders has gained traction since the 1970s, due to their ability to increase the contrast between the fingermark ridge details and deposition surface [5]. Commercially available powders that luminesce in the visible region of the electromagnetic spectrum partially overcome the challenges encountered with multicoloured and/or highly patterned surfaces. However, there are still many surfaces that prove challenging, due to the incorporation of luminescent dyes. The application of NIR luminescent dusting powders has emerged as a potential solution for improving fingermark visualisation and contrast on more challenging surfaces. As a limited number of naturally occurring chemical species exhibit luminescence in the NIR region, potential interferences between the developed fingermarks and their deposition surface are minimised [6]. However, the cost associated with commercially available products limits their use in many jurisdictions, with the two Foster + Freeman® fpNATURAL® Powders, fP Natural 1 and fP Natural 2, costing A$4.80 (€2.98, C$4.38) and A$6.32 (€3.92, C$5.77) per gram respectively [7].

Egyptian blue (EB) is an inorganic pigment first synthesized in ancient Egypt around 3300 BCE [8]. It has been investigated as a potential dusting powder, displaying intense photoluminescent properties when excited with visible light [9]. Attempts to improve the pigment's performance noted a reduction in particle size through exfoliation, followed by lipophilic surface modifications, enhanced the preferential particle adhesion to the fingermark residue [10,11]. The modified pigment proved successful in the effective development of latent fingermarks with reduced background interference and increased fingermark visibility.

In the search for a relatively inexpensive, safe, and accessible dusting powder that improves latent fingermark detection, this study aims to investigate pigments analogous to EB, that satisfy the requirements for

* Corresponding author.
E-mail address: s.lewis@curtin.edu.au (S.W. Lewis).

https://doi.org/10.1016/j.forsciint.2024.112172
Received 8 March 2024; Received in revised form 25 June 2024; Accepted 28 July 2024
Available online 31 July 2024

frugal forensics [12]. This could be defined as low-cost, easily accessible, safe pigments that can be used without any further modifications. Artificial NIR-luminescent pigments that satisfy these criteria include Han blue (HB), a pigment isomorphous with EB, and Han purple (HP), with structures of the three compounds displayed in Fig. 1. The Han pigments originated from ancient China around 800 BCE and their use in ancient artworks prevailed until the end of the Han Dynasty [8,13]. Preliminary studies into their application as latent fingermark development powders provided promising results, prompting the requirement for further research in this domain.

The inorganic copper silicates, EB, HB and HP, have been extensively studied for their impressive optical properties, displaying long luminescent lifetimes and relatively high quantum yields [8]. However, there is ambiguity in the literature concerning these pigments, whose luminescent properties are dependent on a variety of factors, such as the synthesis route, temperature, and reagent ratio, as well as the particle size, the presence of impurities and the deterioration process.

No single study has reported a thorough evaluation of all three pigments, produced under standard commercial routes, and evaluated them using uniform experimental conditions. This is likely attributed to the technically challenging process involved, requiring specialised instrumentation for extensive photoluminescent investigation. Therefore, this study will address this gap, providing an extensive analysis of commercial pigment samples.

The application of the ancient inorganic pigments as luminescent dusting powders for the improved detection of latent fingermarks were evaluated by a pilot study modelled on the recommendations in the International Fingerprint Research Group (IFRG) Guidelines [14]. These studies were conducted with commercial pigments, used without further treatment, and aimed to test the quality of enhancement of fingermarks on non-porous substrates, using glass and polymer banknotes as exemplar surfaces.

2. Materials and methods

2.1. Chemicals

All pigments investigated were commercially procured samples. The pigments of interest included: Egyptian blue (Catalogue No. 10060, Kremer Pigments Inc., Germany, A$2.27/g, €1.41/g) (Langridge Artist Colours, Australia), Han blue (Catalogue No. 10071, Kremers Pigment Inc., Germany, A$0.91/g, €0.57/g) and Han purple (Catalogue No. 10074, Kremers Pigment Inc., Germany, A$2.08/g, €1.29/g). The price of the Kremer pigments was obtained directly from the brand's website [15]. No cost was available for the Langridge pigment, which appears to have been discontinued on the manufacturer's website. The exfoliated Egyptian blue sample was prepared using the Kremer pigment, according to a previously established procedure [11]. The pigment samples were stored in a M-DYCDE-100 Labec Dry Cabinet maintained around 22℃ and 9 % relative humidity.

2.2. Characterisation of synthetic pigments

2.2.1. Optical microscopy

Optical microscopy was used in this study to determine the particle shape and size of the pigments investigated. This was performed using an Alpha300 SAR+ (WITec GmbH, Ulm, Germany) equipped with a 20x/0.4NA objective (Zeiss, Germany). To prepare the samples, a mixture of the pigment suspended in DI water was added to a glass slide and particles were evenly dispersed using centrifugal force. The data obtained was analysed using WITecProjectFOUR (version 4.1.18) ImageJ2 (version 2.14.0/1.54 f). The particle size was estimated as the projected area diameter, and the mean value of 150 randomly selected particulates was reported.

2.2.2. Infrared spectroscopy

Fourier transform infrared (FTIR) spectroscopy was conducted on the pigments using a Nicolet spectrometer (Nicolet iS50, ThermoFisher Scientific, Massachusetts). The instrument was equipped with a tungsten-halogen white light source, KBR beam splitter, and attenuated total reflectance (ATR) crystal. All samples were analysed in solid state over the range of 4000–400 cm^{-1} (64 scans, 4 cm^{-1} spectral resolution). Data was analysed using OPUS software.

2.2.3. Ultraviolet-visible spectroscopy

Ultraviolet-visible (UV-Vis) spectroscopy was used to obtain an absorption spectrum for the pigments of interest. The powders were loaded into the solid-state sample cell with no further preparation and analysed

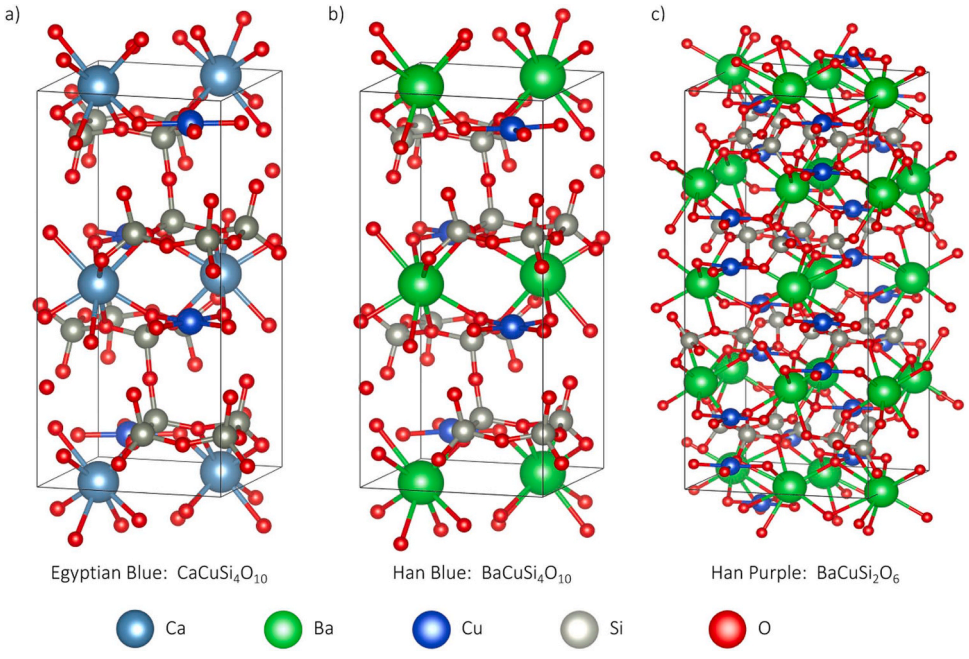

Fig. 1. Crystallographic structure of **(a)** EB, **(b)** HB, and **(c)** HP.

using a Cary 4000 UV-Vis Spectrophotometer (Agilent Technologies, California) set to absorbance mode, across a range of 200–900 nm (1 scan, 2 nm spectral bandwidth). The instrument was equipped with deuterium arc and tungsten halogen lamps (light source changeover at 350 nm) and a baseline correction was conducted using a standard white reflector. Data was analysed using the Cary WinUV software (version 4.20(468)).

2.2.4. Photophysical measurements

Photophysical studies of the pigment were recorded using an FLS980 Photoluminescent Spectrometer (Edinburgh Instruments, UK). For the uncorrected steady-state emission and excitation spectra, the instrument was fitted with a 450 W ozone-free xenon arc lamp, double monochromators for excitation and emission, and Peltier cooled Hamamatsu photomultiplier detectors R928P (185 – 850 nm) and R5509–42 (800 – 1400 nm). The source intensity and emission spectral response were corrected for the emission and excitation spectra by a calibration curve supplied with the instrument. Experimental uncertainties are estimated to be ± 5 nm for the excitation and emission spectra.

Excited state decay measurements of the pigments were conducted using the FLS980 Spectrometer with a microsecond flashlamp. The photoluminescent lifetime was determined by minimising the χ^2 function for the spectral curve fit. Experimental uncertainties are estimated to be ± 8 % for lifetime determinations.

All quantum yields were measured with the use of an integrating sphere and both visible and NIR detectors. To account for differences in detector sensitivity, a correction factor was applied. To obtain the correction factor, a synchronous scan (700 – 800 nm, 0 nm offset) of a blank, inside the sphere, was recorded on both detectors. The integrated spectrum of the NIR detector was then divided by the integrated spectrum of the visible detector to provide the correction factor. Experimental uncertainty is estimated to be ± 20 %.

2.2.5. Supplementary material

Crystallographic structures were obtained from the Cambridge Crystallographic Data Centre, CCDC numbers 1882695, 1632746, and 1623727 for EB, HB, and HP respectively.

This data can be acquired free of charge via https://www.ccdc.cam.ac.uk/, or from the Cambridge Crystallographic Data Centre, 12 Union Road, Cambridge CB2 1EZ, UK; fax: (+44) 1223–336–033; or e-mail: deposit@ccdc.cam.ac.uk.

The structures were interpreted and designed using VESTA software (Version 3) [16].

2.3. Applications in latent fingermark development

2.3.1. Collection of latent fingermarks

Fingermarks were collected in agreement with the Curtin University Human Research Ethics Committee (approval numbers HRE2016–0252 and HRE2023–0127). The experimental design was modelled on the IFRG guidelines [14].

Prior to fingermark deposition, substrates were washed with detergent and DI water, rinsed repeatedly with acetone and DI water, and then left to air dry. KimTech® Science™ KimWipes™ were used to wipe the substrate before deposition to remove any remaining organic residues.

This study used a pool of 5 Donors, aged 20–40. Donors were required to avoid activities that may alter the composition of natural residue present on their fingertips for 30 minutes prior to fingermark deposition. This included washing their hands or the handling of food products, cosmetics, and chemicals. During the fingermark collection process, donors rubbed their fingertips together immediately before deposition, to evenly distribute skin secretions. They were then asked to touch the substrate, establishing contact between the fingertip and the surface, with moderate to light pressure. This contact was maintained for approximately 5 seconds. Following collection, the fingermark samples were stored in an air-conditioned laboratory covered from direct sunlight. The temperature and relative humidity of this environment were previously established as 20 – 23 ℃ and 28 – 67 %, respectively, using a Digitech QP-6013 data logger [17].

A combination of depletion series and split fingermark samples were used in this study. To obtain a depletion series, donors were asked to deposit 3 – 6 consecutive fingermarks, using the same finger(s) in immediate succession (Fig. 2a). For split-print samples, donors were asked to touch the substate with their middle three fingers (ring, middle and index), simultaneously (Fig. 2b). The substrate was cut in half prior to development, with each half considered a single entity for grading purposes.

2.3.1.1. Pilot Study 1. Fingermarks were deposited onto A4 glass panels from certificate frames (Lifestyle Brands, Australia). The 5 donors were asked to provide 5 depletions of 10 fingermarks, one for each finger, accumulating a total of 250 fingermarks per pigment. Samples were left in ambient conditions for 72 hours prior to development.

2.3.1.2. Pilot Study 2. Substrates used were selected for their designs that could impact latent fingermark visualisation and included polymer bank notes.

Twenty dollar and five dollar Australian polymer banknotes were used as a more challenging substrate. The twenty dollar notes used in this study included circulated first-generation polymer banknote design. Both circulated and uncirculated five dollar notes from the second-generation design were used. The 5 donors provided both depletion series (3 depletions on twenty dollar notes and 6 depletions on five dollar notes) and split-print fingermarks for analysis. The location of fingermark deposits on the bank notes was varied to account for surface heterogeneity. However, deposits on areas known to incorporate security features were purposefully avoided where possible.

Samples were stored under ambient conditions for 48 hours prior to development. Permission was granted by the chief scientist of the Reserve Bank of Australia (RBA) for the use and damage of uncirculated and circulated polymer banknotes.

2.3.2. Development of latent fingermarks

Fingermarks were developed using a dusting technique, with the ancient pigments in dry powder form. Soft, low-density disposable fibreglass brushes (TheBreeze, USA) were used to apply the powder to the deposited fingermark [5]. Samples were brushed using a slow swirling motion, following the direction of the ridge details, to prevent damage to the fingermark [5,10].

2.3.3. Photography of latent fingermarks

Developed fingermarks were photographed using a Canon camera (EOS 40D, Canon, Japan), which was modified to photograph in the infrared (IR) region by the removal of the internal IR blocking filter and used in conjunction with an IR Black-Red filter (B & W IR lens filter, 830/093). The camera was equipped with a Canon EFS 18–55 mm lens and mounted to a Firenze mini repro stand with a desktop computer connection for remote shooting, using the Canon EOS Utility (Version 2.0) software. The aperture and shutter speed were selected to enhance fingermark visibility. During photography, samples were illuminated by a square array of white light (Mirabella, 4000 K 14 W LED) and a 500Watt xenon arc lamp forensic light source (Rofin Polilight® PL500, Rofin, Australia), with a white light optical output (400–680 nm).

2.3.4. Fingermark grading

Fingermarks were graded based on the visual examination of photographed samples, with no digital processing used to enhance contrast. A single assessor, with approximately six months of prior experience, graded fingermarks using a five-point scale adapted from the UK Home Office Centre for Applied Science and Technology (CAST) [14,18].

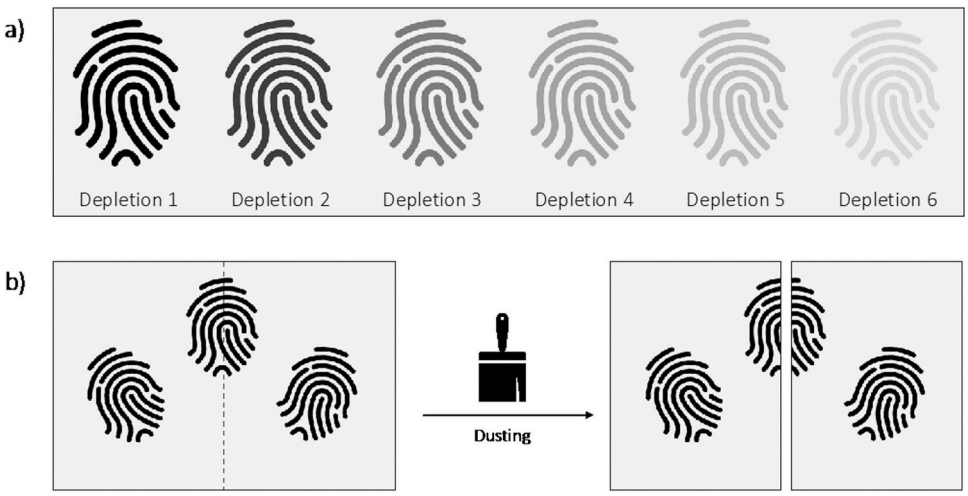

Fig. 2. Schematic of fingermark depositions for **(a)** depletion series and **(b)** split-print fingermarks.

Fingermarks received a score from 0 to 4 based on the degree of ridge detail development and contrast against the substrate, as outlined in Table 1. Samples graded 3 or above were considered 'suitable' for forensic applications, whereas those graded a 1 or 2 were deemed 'unsuitable', and those that received a 0 grade were denoted as 'undetected'.

Table 1
Fingermark grading scheme used in this investigation.

Grade	Friction Ridge Detail	Contrast	Example
0	No development.	No contrast	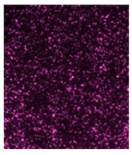
1	< 1/3 of continuous ridge detail, some evidence of contact.	Poor contrast	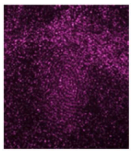
2	1/3 – 2/3 of the developed fingermark is continuous ridge detail.	Moderate contrast	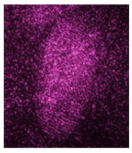
3	> 2/3 of the developed fingermark is continuous ridge detail.	Good contrast	
4	Full development; whole fingermark visible with continuous ridges.	Excellent contrast	

3. Results and discussion

3.1. Characterisation of synthetic pigments

Commercial EB pigments manufactured by Langridge Artist Colours and Kremer Pigments Inc. (EB-L and EB-K, respectively), as well as HB and HP pigments from Kremer Pigments Inc. (Fig. 3), were studied for their physical properties, with assessments into the pigment particle size, chemical structure and optical properties explored. Two EB pigment suppliers were selected for this study to investigate the variability in physical properties between different commercially available samples of the same product.

EB ($CaCuSi_4O_{10}$) and HB ($BaCuSi_4O_{10}$) are isostructural alkaline-earth metal copper tetrasilicates, with crystallographic lattices comprised of analogous nanosheets, arranged in layers (Fig. 4a-b) [8,19–23]. The nanosheets contain eight-membered rings of corner-shared silica tetrahedron ($[SiO_4]^{2-}$), whereby each silica atom is bound to two adjacent silica atoms in the same ring, by equivalent bridging oxygens, and a neighbouring tetrahedron belonging to a separate Si_4O_{10} ring structure, by an inequivalent bridging oxygen. The fourth oxygen in the silica tetrahedron is an anionic non-bridging oxygen, that coordinates to a chromophoric Cu^{2+} ion. The copper ions are coordinated to four non-bridging oxygens, each from a separate Si_4O_{10} ring, with each Cu-O bond equivalent and arranged in a near-perfect square planar geometry (D_{4h} symmetry, space group *P4/ncc*) [8,19,21,24–26]. This symmetry is due to the tetragonal distortion that occurs for metals in the d^9 configuration bonded to identical ligands, known as the Jahn-Teller effect [24]. The alkali-earth metal bridges the nanosheets $[CuSi_4O_{10}]^{2-}$ in a distorted cubic geometry. The change in the bridging metal from Ca^{2+} to Ba^{2+} between EB and HB respectively, increases the stacking distance between adjacent nanosheets [8,19,21,22]. Additionally, a marginal

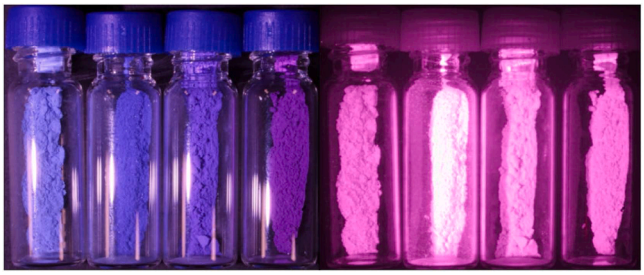

Fig. 3. EB-L, EB-K, HB, and HP respectively, pictured (left) under natural light (f/22, 1/125 s) and (right) under white light in NIR luminescence mode (f/29, 1.0 s, B & W IR lens filter).

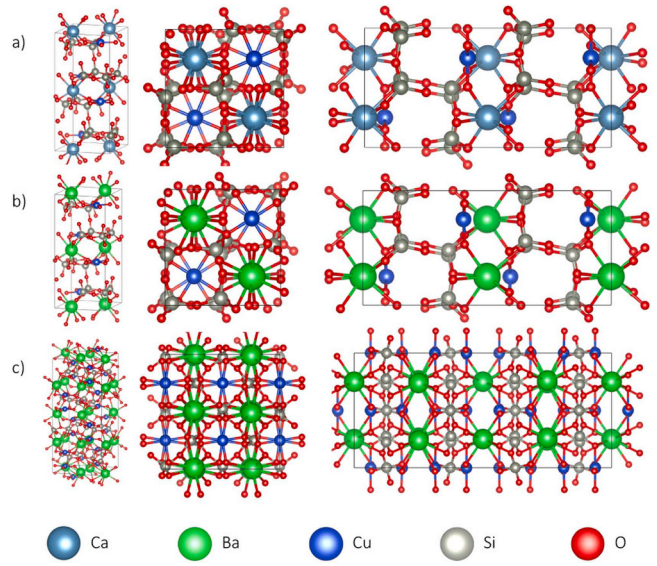

Fig. 4. Crystallographic structure of **(a)** EB, **(b)** HB, and **(c)** HP.

decrease in Cu-O bond distance is likely attributed to the increase in the atomic radii of the alkali earth metal. However, the quoted bond lengths for each structure vary slightly between sources, with values ranging between 1.91 – 1.928 Å for EB and 1.918 – 1.925 Å for HB.

The crystallographic structure of HP ($BaCuSi_2O_6$) differs from that of HB, due to the arrangement and quantity of silica tetrahedrons in the compound (Fig. 4c) [8,19]. In HP, the silica tetrahedrons form isolated square ring structures, corner linked by non-bridging oxygen atoms bonded to the Cu^{2+} ion in a near-perfect square planar geometry. The copper ions are arranged in CuO_4-CuO_4 dimers, with a square lattice arrangement, resulting in antiferromagnetic coupling [8]. Much like HB, the structure of HP consists of analogous nanosheets bridged by the Ba^{2+} alkali-earth metal.

The samples were analysed via optical microscopy, to assess the particle size in contrast to the advertised value. The pigment suppliers advertise EB as approximately 50 μm (Langridge) and < 120 μm (Kremer), whereas the average measured particle sizes were 27 μm (σ = 14.9 μm) and 29 μm (σ = 32.6 μm), respectively. For HB and HP Pigments, Kremer Inc. advertises a particle size < 40 μm. The measured mean values were within this range, calculated as 17 μm (σ =10.5 μm) for HB and 14 μm (σ = 6.2 μm) for HP. This is consistent with visual observations of particle size and shape under the optical microscope, as shown in Fig. 5. However, difficulties in elucidating the particle size arose from the ineffective distribution of the pigment on the microscopy slide. Studies conducted by Errington *et al.* [10] uncovered that the quality of latent fingermarks developed improved when the particle size of EB was reduced from 40 μm to 5 μm, with improved adhesion between the pigment particles and fingermark residue. Hence, the smaller particle size of HB and HP may overcome the requirement for modifications to the commercial sample. This would be advantageous, as the use of the pigment without further treatment supports frugal forensic applications [12].

A comparison between FTIR spectra collected for the four pigments of interest is displayed in Fig. 6, with the assignment of key vibrational modes indicated in Table 2. The two EB pigments displayed similarities in the peak signals in the spectra, aside from a signal at 790 cm^{-1} that was not observable in the EB-K spectrum. The peaks measured were also consistent with other literary reports, confirming the identity of the alkali-earth copper tetrasilicate [25,26]. The two samples showed large variations in the peak intensities, however, this could potentially be explained by the variation in particle size, whereby the decrease in particle size of inorganic compounds has been linked to an increase in FTIR signal intensity. The spectra for HB displayed many commonalities with the EB samples, asides from the presence of a signal at 1474 cm^{-1} and 924 cm^{-1}. The spectrum of HP has signals in the same general region as EB and HB, due to Si-O-Si symmetric and asymmetric stretching, occurring between 1230 cm^{-1} and 420 cm^{-1}. Though, it is likely that variations in the number of signals and their intensity can be related to the different crystallographic structures of the compound.

The photophysical properties of the four pigments were analysed, with the absorption, emission, luminescent lifetime, and quantum yields recorded for samples in solid state under ambient conditions.

The inorganic copper silicates display square planar geometry around the Cu^{2+} centre, inducing a descent in symmetry from O_h (octahedral) to D_{4h} (square-planar) [8,19,24]. Broadband absorptions between 500 nm and 900 nm were observed for the pigments, correlating to the following d-d ligand-field transitions centred on the copper: $^2B_{1g} \rightarrow {}^2A_{1g}$, $^2B_{1g} \rightarrow {}^2E_g$, $^2B_{1g} \rightarrow {}^2B_{2g}$ (Fig. 7). The $^2B_{1g} \rightarrow {}^2B_{2g}$ transition is responsible for the NIR emission observed upon radiative decay to the ground state. Both EB pigments provided similar absorption spectra, whereas the Han pigments displayed a blue-shift in the wavelength of the peak absorbances, observed to a greater extent for HP than HB.

Photoluminescent emission spectra were obtained using an excitation wavelength of 627 nm (Fig. 8), corresponding to the $^2B_{1\,g} \rightarrow {}^2E_g$ electronic transition. The emission for both EB samples spanned from 800 – 1200 nm, with a peak wavelength of 912 nm consistent between the two samples. This value falls within the range of literary reported values, spanning from 909 – 950 nm [8,19,27–29]. HB is isomorphous to EB and displayed a red-shifted emission band, centred around 951 nm. This aligns with the reported values between 948 – 980 nm [8,19,28,29]. The red-shift is attributed to the different crystal field splitting caused by the substitution between the Ca^{2+} and Ba^{2+} ions [8]. On the other hand, the emission spectrum of HP was found to be analogous to those of EB, with maximum centred at 902 nm.

This value varies from previous studies, where Pozza *et al.* [19] quotes 980 nm as the wavelength at maximum emission and 924 – 925 nm is reported in other sources [19,28,30].

A relatively long luminescent lifetime was observed for all four pigment samples, as typical of parity-forbidden ligand-field transitions (Table 3) [31,32]. These values are consistent with previous reports. The excited state lifetime decay of EB-L was best fit using a biexponential

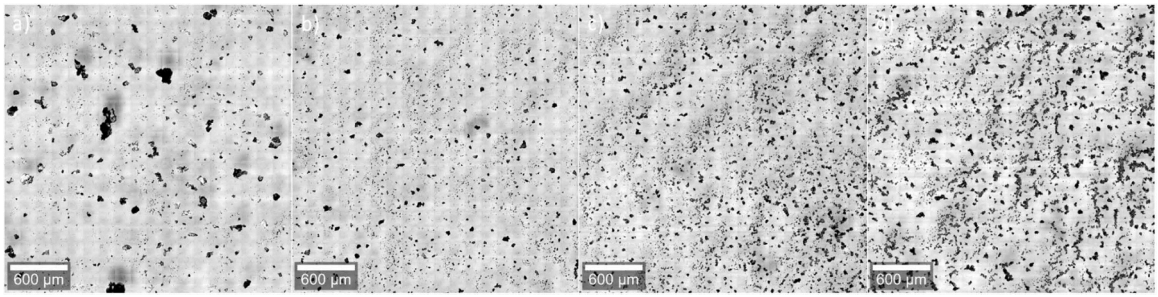

Fig. 5. Optical microscopy of **(a)** EB-K, **(b)** EB-L, **(c)** HB, and **(d)** HP.

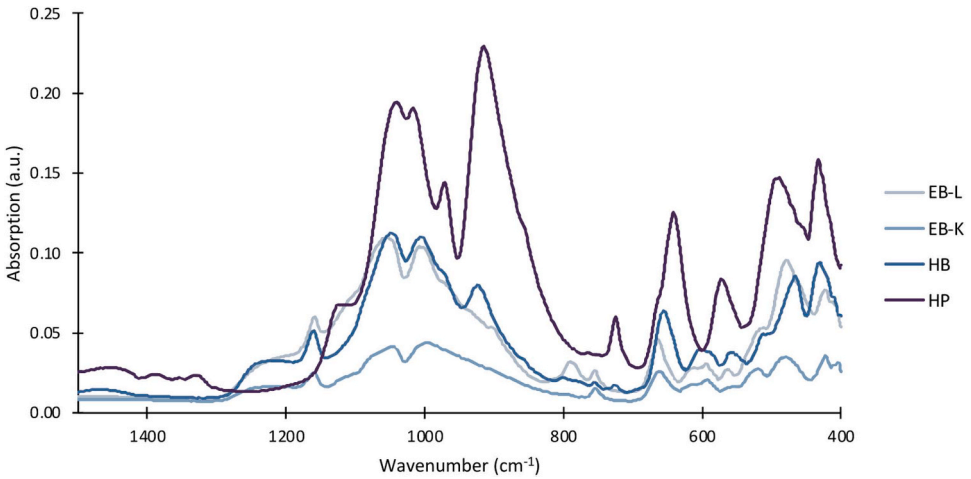

Fig. 6. ATR corrected FTIR spectra of EB, HB and HP.

Table 2
Functional group assignment for vibrational modes observed in the ATR corrected FTIR of EB, HB, and HP.

Pigment	Peak Wavenumber (cm^{-1})	Assignment
Egyptian blue - L	479	Si-O-Si bending
	594, 663, 755, 790	Si-O-Si symmetric stretch
	1007, 1054, 1159	Si-O-Si asymmetric stretch
Egyptian blue - K	484	Si-O-Si bending
	593, 662, 755	Si-O-Si symmetric stretch
	996, 1047, 1166	Si-O-Si asymmetric stretch
Han blue	467	Si-O-Si bending
	656	Si-O-Si symmetric stretch
	1006, 1049, 1160, 1226	Si-O-Si asymmetric stretch
	557	Cu-O symmetric stretch
	598	Cu-O asymmetric stretch
Han purple	433, 495, 725, 916	Si-O-Si symmetric stretch
	1017, 1041, 1123, 1328	Si-O-Si asymmetric stretch
	572	Cu-O symmetric stretch
	641	Cu-O asymmetric stretch

function, whereas all Kremer Inc. pigments presented monoexponential decays. Compared to the other pigments, HP displayed a notably shorter luminescent lifetime, potentially attributed to its differing crystallographic structure and space group or the presence of quenching impurities. As prior literature postulates that the synthesis route and particle size alter the lifetime measurements obtained, without substantiating evidence to justify the claim, it is difficult to appropriately compare the results obtained [8].

The two EB pigments displayed different values of photoluminescence quantum yields: 6.16 % (Langridge) and 14.75 % (Kremer Inc.). These values are close to literature reports of 10.5 % [8,27]. On the other hand, the quantum yields for HB and HP were measured at 16.67 % and 5.17 %, respectively. Hydrothermally synthesized HB and HP pigments were reported with lower quantum yields, 6.9 % and 0.9 %, respectively [25].

The photophysical properties of the four pigments assessed are summarised in Table 3. The data obtained provides an overview of the photophysical properties measured under consistent conditions. The results justify the pigments' potential use as luminescent dusting powders for the detection of latent fingermarks, with emissions in the NIR region of the electromagnetic spectrum, long luminescent lifetimes, and good quantum efficiency. Additionally, the smaller commercial particle size of HB and HP could potentially allow for the application of the pigments without the requirement for further treatments.

3.2. Applications to latent fingermark development

3.2.1. Pilot study 1

The aim of this study was to conduct a preliminary proof of concept to assess the suitability of HB and HP as luminescent dusting powders. The development of latent fingermarks deposited on a glass substrate was investigated to evaluate their ability to enhance fingermark residues for effective visualisation, without additional treatment to the commercial product.

Latent fingermarks developed using HB and HP displayed similar performance for their ability to visualise fingermarks suitable for use in forensic investigations. Fig. 9 displays a comparison between the proportion of suitable fingermarks developed using HB and HP, with a grade of three or above awarded to the majority of samples developed by both pigments. However, HB displayed marginally better performance, as a greater affinity for the fingermark residue was observed.

A comparison between development success and the fingermark depletion number indicates a minimal effect on the proportion of suitable fingermarks (Fig. 10). This implies that the Han pigments are sensitive dusting powders, showing an affinity for the deposited fingermark residues. This is a promising result as it reflects the ability of the pigment to develop fingermarks containing various amounts of latent residues, an ideal quality for forensic applications.

Not unexpectedly, the results indicated donor variability (Fig. 11), with a higher proportion of unsuitable results from donor 5.

Based on this pilot study, it could be concluded that HB and HP are capable of developing latent fingermarks with sufficient contrast, required for effective visualisation. The majority of developed fingermarks assessed in this study could be deemed suitable for use in forensics applications. However, the greatest cause for lower grading pertained to the quality of fingermark deposit, owing to donor variability, with a decrease in effective visulisation exacerbated by the pigments coating the substrate. Overall, it was determined that HB outperformed HP, with increased selectivity towards the deposited fingermark residues.

3.2.2. Pilot study 2

This study was conducted to assess the performance of HB and HP pigments to enhance fingermark visualisation on highly patterned, multicoloured or reflective surfaces. Polymeric banknotes were selected as a substrate known to be challenging for fingermark visualisation due to the semi-porous nature of the polymeric coating, security features that alter surface characteristics, and surface texture defects caused by degradation of the polymeric coating and general wear and tear [33-35]. Security features, including a transparent window, tactile enhancements, foil stamping and luminescent dyes, introduce variability in the surface characteristics and colours of the banknote [34,36]. Notably, the

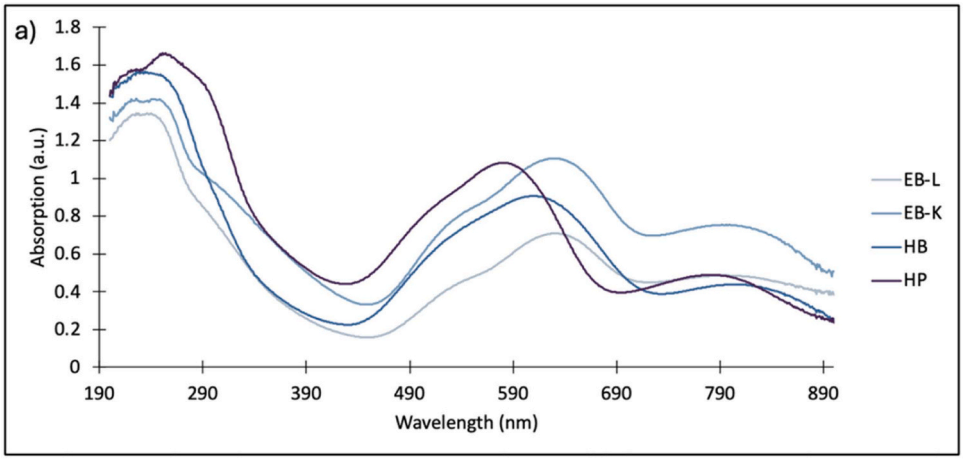

c)

Energy Transition	Wavelength (nm) EB-L	EB-K	HB	HP
$^2B_{1g} \rightarrow {}^2A_{1g}$	~ 556	~ 554	~ 552	~ 532
$^2B_{1g} \rightarrow {}^2E_g$	630	628	610	581
$^2B_{1g} \rightarrow {}^2B_{2g}$	796	796	799	783

Fig. 7. **(a)** Absorption spectra of the four silicate pigments, **(b)** the energy level diagram for the Cu(II) centre [23], and **(c)** the assignment of absorption wavelength to energy level transitions.

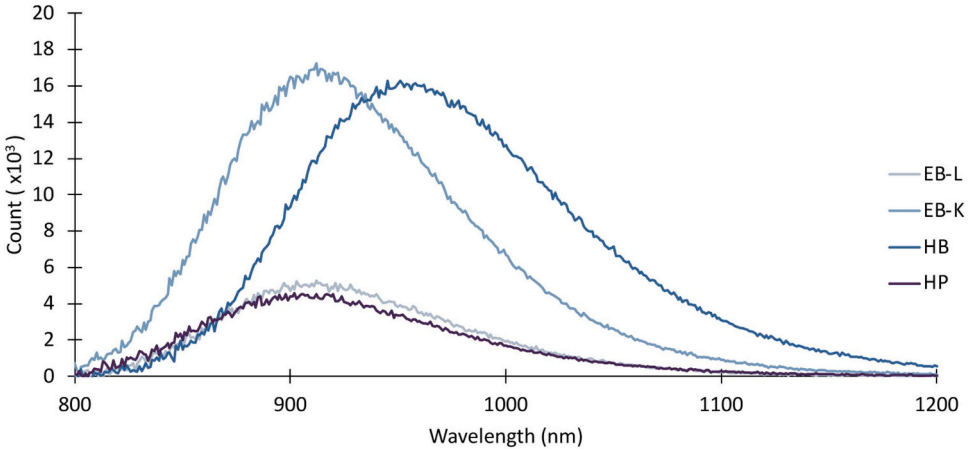

Fig. 8. Emission spectra of EB, HB, and HP.

application of inks within the polymeric structure has been identified to introduce inconsistencies, with an uneven coating and the presence of impurities producing random disparities in the surface characteristics [36]. This makes fingermark visualisation inherently challenging, as it alters the interaction between the deposited fingermark and the banknote components [35].

HB and HP were used to develop a series of 6 fingermark depletions, collected on second-generation five dollar polymer banknotes. A large proportion of the fingermarks developed were classed as unsuitable for use in forensic applications, due to poor contrast, resulting from the pigment coating the substrate. Comparatively, HP developed more suitable fingermarks than HB, with better selectivity towards the fingermark residue observed, resulting in less pigment coating on the substrate, allowing for the visualisation of continuous ridge details. Additionally, the grades allocated to fingermarks decreased in accordance with the depletion series, indicating a degree of sensitivity in the performance of the pigments as fingermark dusting powders (Fig. 12).

Elevated background interferences further reduced the contrast between developed fingermarks and the substrate, lowering the grades awarded. It was identified that an anti-counterfeit security feature of the banknotes is an ink that emits in the NIR region, much like the Han pigments. As this study used a broadband light source to excite the pigments into a luminescent state, it was hypothesised that this interference could be potentially mitigated by using a light wavelength of lower energy, to prevent the excitation of the dye. However, this was disproven, with the ink remaining visible under a range of excitation wavelengths (350 nm – 650 nm). That said, some degree of the total background interference was minimised by exclusively using a longer

Table 3
Summary of photophysical data collected for commercial EB, HB, and HP pigments.

Compound	Absorption Properties	Emission Properties			
	λ abs	λ em	Φ	τ	
	(nm)	(nm)	%	(μs)	χ^2
Egyptian blue (L)	796, 630, 556	912	6.16	36.89 (43 %) 106.85 (57 %)	1.149
Egyptian blue (K)	796, 628, 554	912	14.75	138.49	1.039
Han blue	799, 610, 552	951	16.67	152.59	1.015
Han purple	783, 581, 532	902	5.17	21.6	1.01

wavelength. While this is advantageous for improved visualisation, it renders this technique inapplicable to forensic departments not equipped with a specialised light source and therefore does not satisfy the conditions of frugal forensics.

Comparative assessments of the pigments on polymer banknotes were conducted through the development of split print impressions, generating a side-by-side comparison between development methods. This provided insight into their relative competencies in developing fingermarks, with sufficient contrast, and resolution of ridge details. The performance of the Han pigments was assessed against exfoliated Egyptian Blue (eEB), previously reported by Shahbazi and co-workers [11,17].

Overall, HP was identified as the most successful candidate for NIR luminescent fingermark dusting, outperforming both HB and eEB (Fig. 13). Whilst the luminescence of HP was less apparent in contrast to the blue pigments, the smaller particle size resulted in a higher resolution fingermark with evident ridge details. The performance of HB was akin to HP, however, continuous ridge details were observed less consistently for fingermarks developed with this pigment due to the larger particle size. Comparatively, eEB displayed minimal selectivity for the deposited residues, with an excessive coating of the substrate observed in all samples. This distorted the appearance of continuous ridge details, causing few fingermarks to be graded above a 2.

A disparity in results for Pilot Study 1 and Pilot Study 2 was noted, with HB yielding the best results on the glass substrate and HP on the polymer banknotes. This could be attributed to the increased porosity

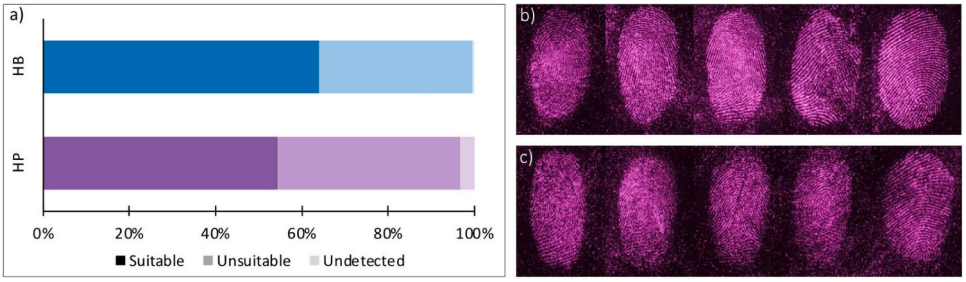

Fig. 9. **(a)** Comparison between latent fingermarks developed using HB and HP (n = 250, f/16, 1.0 s). **(b)** Fingermarks developed using HB (donor 4, depletion 1, fingermarks 1–5). **(c)** Fingermarks developed using HP (donor 4, depletion 1, fingermarks 1–5).

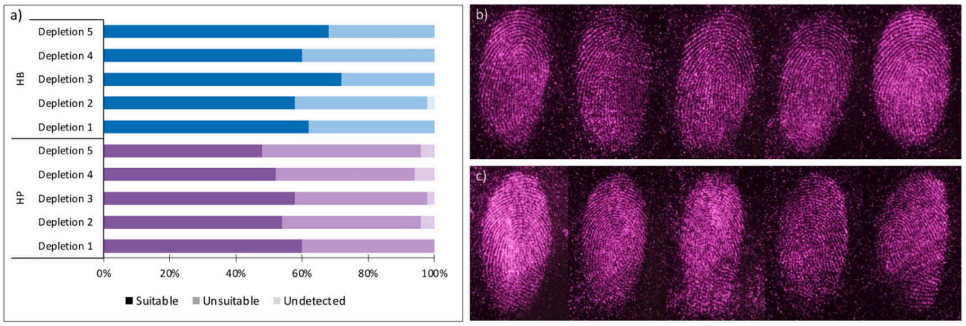

Fig. 10. **(a)** Graphical representation of sensitivity assessment of Han pigments as latent fingermark dusting powder (f/16, 1.0 s), based on the grades awarded for each depletion (n = 50). Examples of developed fingermark depletion series (Donor 4, fingermark 10, depletion 1–5) for **(b)** HB and **(c)** HP.

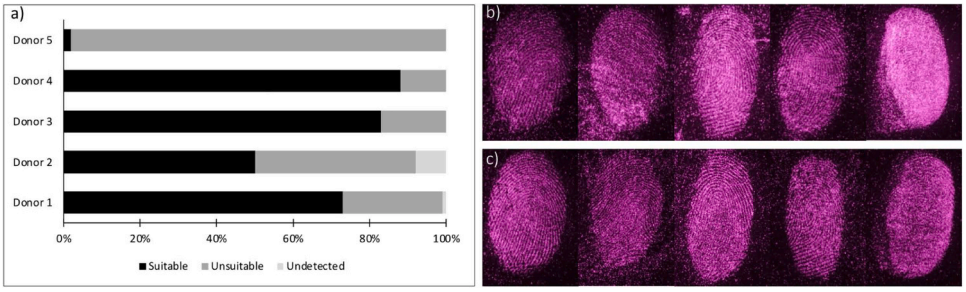

Fig. 11. **(a)** Graphical relationship between the suitability of developed fingermarks of HB and HP inclusive and the donors (f/16, 1.0 s). Examples of fingermarks developed (depletion 1, fingermark 1) for donors 1–5 (left to right), developed with **(b)** HB and **(c)** HP.

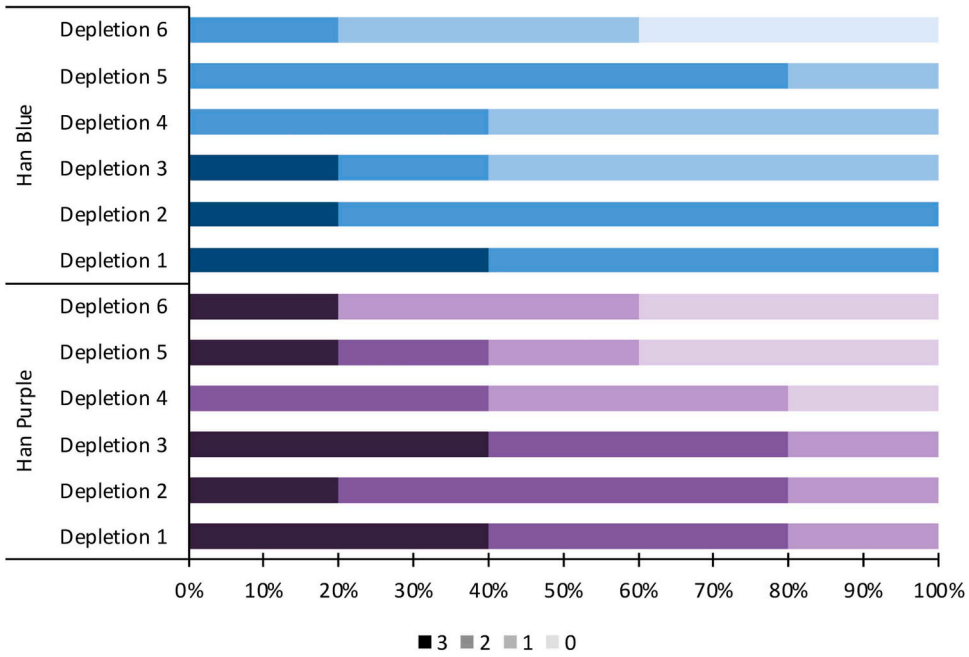

Fig. 12. Grades awarded to fingermark depletions (n = 5) deposited on five dollar polymer banknotes, developed using the Han pigments (f/11, 1.0 s).

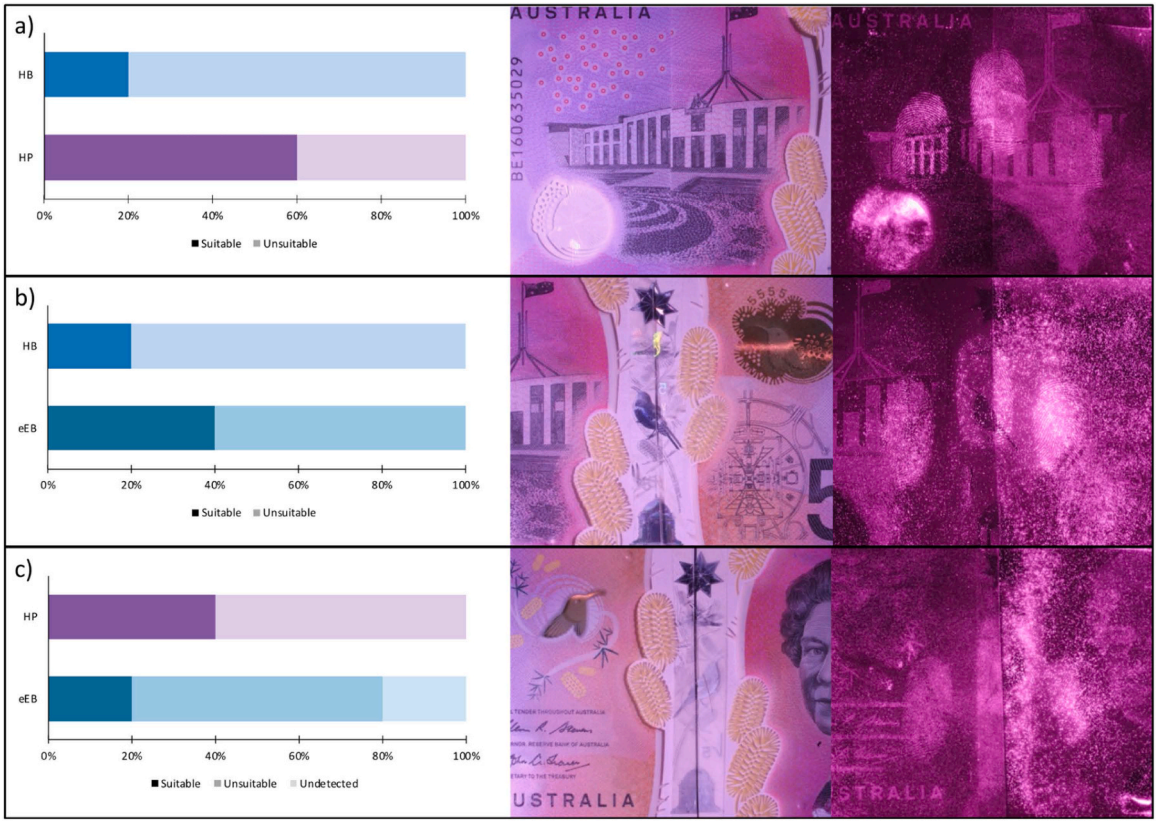

Fig. 13. Comparative assessment of split-print fingermarks (n = 5) (left) and photographs of the developed split-print fingermarks under natural lighting (f/20, 1/800 s) (middle) and under a white broadband light source in NIR luminescence mode (f/11, 2 s, B & W IR lens filter) for **(a)** HB (left) and HP (right), **(b)** HB (left) and eEB (right), and **(c)** HP (left) and eEB (right).

and surface texture of the polymer banknotes, compared to the glass substrate.

The development of latent fingermarks on twenty dollar polymer banknotes was deemed unsuccessful, with all collected fingermarks receiving a 0 grade. Both HB and HP pigments coated the background substrate, showing no affinity for the fingermark residue (Fig. 14). This was potentially caused by ineffective substrate cleaning and preparation, or the rougher surface texture observed in the first-generation

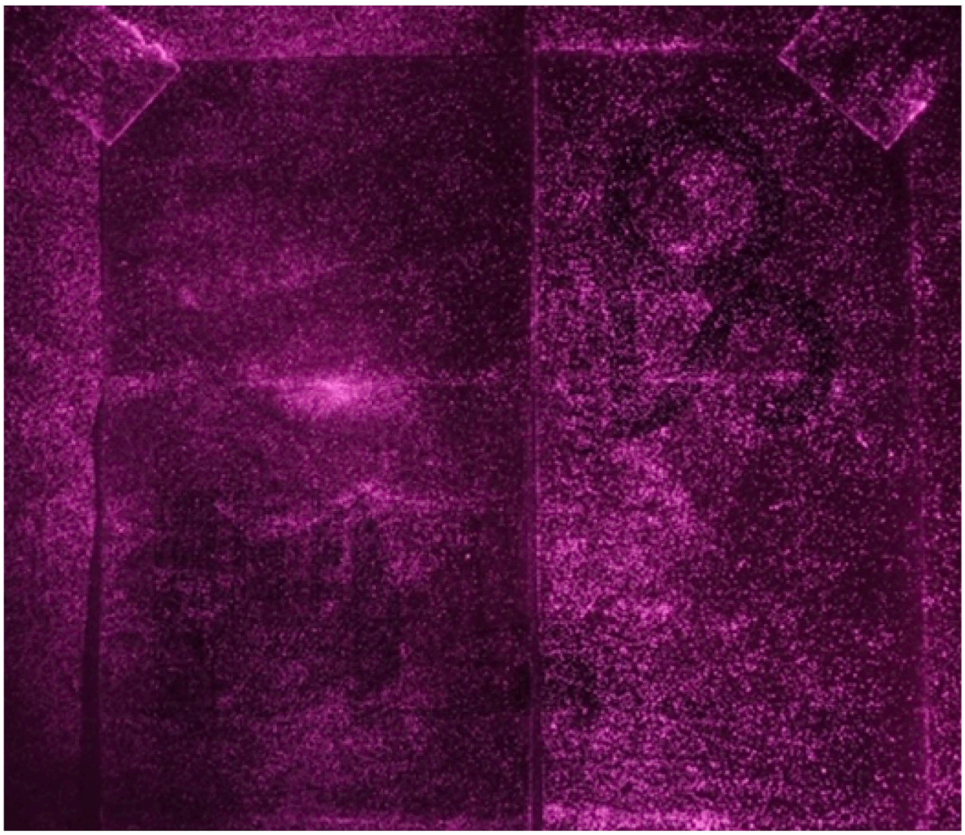

Fig. 14. Split-print fingermarks developed using HP (left) and HB (right) on twenty dollar polymer banknotes.

circulated polymer banknotes. However, more likely this is attributed to the elevated surface roughness of the banknote polymeric coating, resulting from their handling [33].

3.2.3. *Experimental considerations*

There are a variety of factors that could potentially explain the observed inconsistencies in fingermark development ability for the three pigments.

During the Pilot Study 1, the pigments were observed to inconsistently coat the background substrate, showing minimal affinity for the fingermark residue. A separate study conducted by Shahbazi *et al.* [11,17] indicated that this issue could be minimised by coating the pigment with lipophilic polymers. It was found that this increased selectivity towards the deposited fingermark residues, mediated by lipophilic interactions with the sebaceous skin secretions. While this would be logical continuation to this investigation, the treatment of the commercially purchased pigments reduces its applicability for frugal forensics.

It was noted that the background substrate coating correlated to residues remaining on the substrate surface following the cleaning process. This was due to wearing of nitrile gloves, which were degraded by acetone during the washing process. Kimtech® Science™ Kimwipes™ were found to effectively combat this issue and remove any residues remaining on the substrate post-drying, decreasing the extent of the pigments coating the substrate. However, it is worth considering that latent fingermarks of interest in forensic investigations are unlikely to be deposited onto an ideal, clean substrate. Hence, this provides a true indication of the limitations of this technique for its "real-world" intended purpose.

The experience of the individual carrying out the dusting is another factor that influences the effective enhancement of fingermark ridge details. While this study used a single person, further studies incorporating multiple fingermark dusters from a range of expertise backgrounds would be required to provide evidence of the robustness of this technique. Moreover, further investigations into the powdering technique, such as the type of dusting brush used, could prove advantageous in improving the performance of the pigments as fingermark dusting powders.

Additionally, it is important to note that fingermark grading can be considered a subjective process [37,38]. Using a grading scale, as outlined in Table 1, and following the IFRG guidelines pertaining to the assessment and reporting of samples, this variation can be minimised but not entirely eradicated [14,37]. The grading scale used in this study considered the amount of visible ridge detail and the contrast between the developed fingermark and the substrate equally. This approach was taken to ensure that the results reflected the pigment's ability to selectively develop the fingermark residues, accounting for the quality of the mark deposited. This is a key challenge associated with donor variation, whereby skin secretion chemistry, deposition pressure, movement and contact time could impact the quality of the fingermark obtained [5,14,18,39,38]. It is recommended that further studies, graded by multiple fingermark assessors, would be beneficial in validating the results obtained, reducing subjectivity in the grades awarded through moderation.

4. Conclusion

This study has completed a thorough investigation into the physical properties of Egyptian blue, Han blue and Han purple artistry pigments, commercially produced by Kremer Pigments Inc. and Langridge Artist Colours.

Preliminary studies into their applicability as latent fingermark dusting powders provided promising results, indicating a degree of selectivity to the deposited fingermark residues. However, poor contrast was consistently observed in studies conducted using polymer banknotes as the substrate, likely due to the changes that occur within the

polymeric coating over time. This results in a degree of porosity that limited the amount of fingermark secretions remaining on the surface following the aging period.

It can be hypothesised that alternate fingermark dusting techniques, such as the use of non-synthetic dusting brushes in combination with using a clean brush to carefully remove excess pigment on the substrate surface would improve the contrast of the developed fingermarks. Moreover, applying a lipophilic coating onto the raw pigment would likely improve its affinity to the sebaceous fingermark residues, resulting in more consistent development of continuous ridge details. This has proved successful in prior studies on Egyptian blue, and would therefore be a logical extension to the work conducted with Han blue and Han purple.

Overall, this study has identified that Han blue and Han purple display the photophysical properties to suggest that they are a workable fingerprint dusting alternative to Egyptian blue, at a lower price. The work demonstrates the successful application of powders as received in some common instances of forensically relevant fingerprint evidence. These pigments should be further investigated for "off the shelf" application as well as more technologically advanced modifications to improve luminescent fingerprint dusting powders, such as particle size optimization and lipophilic surface coatings.

CRediT authorship contribution statement

Ruby La Rocca: Conceptualization, Methodology, Investigation, Visualisation, Writing – original draft, Writing – review & editing. **Rebecca Pitman**: Methodology, Investigation, Writing – review & editing. **Sorour Shahbazi**: Conceptualization, Methodology, Investigation, Writing – review & editing. **Thais Lópes**: Methodology, Investigation, Writing – review & editing, Supervision. **Elena Dallerba**: Conceptualisation, Investigation, Writing – review & editing, Supervision. **Massimiliano Massi**: Conceptualisation, Writing – review & editing, Supervision. **Gregory D. Smith**: Conceptualization, Writing – review & editing. **Simon W. Lewis**: Conceptualization, Visualisation, Writing – review & editing, Project administration, Supervision.

Declaration of Competing Interest

The authors declare that they have no known competing financial interests or personal relationships that could have appeared to influence the work reported in this paper.

Acknowledgements

The authors would like to thank all fingermark donors who took part in this study. Lee Cameron (Curtin University) is thanked for assistance with collection of luminescence spectra and review of drafts of the manuscript. Sorour Shahbazi was supported by a Research Training Program Stipend Scholarship awarded by Curtin University and Thais Lópes is supported by a Curtin ATN-South American Scholarship. Ethics approval for this study was granted by the Curtin University Human Research Ethics Committee (approval numbers HRE2016–0252 and HRE2023–0127).

References

[1] R.S. King, P.M. Hallett, D. Foster, NIR-NIR fluorescence: A new genre of fingermark visualisation techniques, Forensic Sci. Int 262 (2016) e28–e33, https://doi.org/10.1016/j.forsciint.2016.03.037.
[2] G.S. Sodhi, J. Kaur, Powder method for detecting latent fingerprints: a review, Forensic Sci. Int. 120 (3) (2001) 172–176, https://doi.org/10.1016/S0379-0738(00)00465-5.
[3] C. Lennard, The detection and enhancement of latent fingerprints, US Dep. Justice (2001) D2–D88.
[4] T. Poletti, L.M. Berneira, L.F. Passos, B.N. da Rosa, C.M.P. de Pereira, Kd. C. Mariotti, Preliminary efficiency evaluation of development methods applied to aged sebaceous latent fingermarks, Sci. Justice 61 (4) (2021) 378–383, https://doi.org/10.1016/j.scijus.2021.03.007.
[5] B. Yamashita, M. French, Fingerprint Sourcebook. Chapter 7: Latent Print Development, US Dept of Justice, Office of Justice Programs, National Institute of Justice, 2010.
[6] P. Maynard, J. Jenkins, C. Edey, et al., Near infrared imaging for the improved detection of fingermarks on difficult surfaces, Aust. J. Forensic Sci. 41 (1) (2009) 43–62, https://doi.org/10.1080/00450610802172248.
[7] fpNATURAL® Powders. Latent Forensics. 2024. Accessed June 20, 2024. ⟨https://latentforensics.com/products/fpnatural%C2%AE-powders⟩.
[8] M. Nicola, R. Gobetto, A. Masic, Egyptian blue, Chinese blue, and related two-dimensional silicates: from antiquity to future technologies. Part A: general properties and historical uses, Rend. Lince-.-. Sci. Fis. e Nat. 34 (2) (2023) 369–413, https://doi.org/10.1007/s12210-023-01153-5.
[9] G. Verri, The spatially resolved characterisation of Egyptian blue, Han blue and Han purple by photo-induced luminescence digital imaging, Anal. Bioanal. Chem. 394 (4) (2009) 1011–1021, https://doi.org/10.1007/s00216-009-2693-0.
[10] B. Errington, G. Lawson, S.W. Lewis, G.D. Smith, Micronised Egyptian blue pigment: a novel near-infrared luminescent fingerprint dusting powder, Dyes Pigments 132 (2016) 310–315, https://doi.org/10.1016/j.dyepig.2016.05.008.
[11] S. Shahbazi, J.V. Goodpaster, G.D. Smith, T. Becker, S.W. Lewis, Studies into exfoliation and coating of Egyptian blue in methanol for application to the detection of latent fingermarks, Sci. Justice 62 (4) (2022) 455–460.
[12] J.T. Bouzin, T. Lópes, A.L. Heavey, J. Parrish, G. Sauzier, S.W. Lewis, Mind the gap: the challenges of sustainable forensic science service provision, Forensic Sci. Int.: Synerg. 6 (2023) 100318, https://doi.org/10.1016/j.fsisyn.2023.100318.
[13] H. Berke, The invention of blue and purple pigments in ancient times, Chem. Soc. Rev. 36 (1) (2007) 15–30.
[14] International Fingerprint Research Group, Guidelines for the assessment of fingermark detection techniques, J. Forensic Identif. 64 (2) (2014) 174–200.
[15] Pigments. Kremer Pigmente. Accessed June 20, 2024. ⟨https://www.kremer-pigmente.com/en/shop/pigments/⟩.
[16] K. Momma, F. Izumi, VESTA: a three-dimensional visualization system for electronic and structural analysis, J. Appl. Crystallogr. 41 (3) (2008) 653–658.
[17] S. Shahbazi, J.V. Goodpaster, G.D. Smith, T. Becker, Preparation, characterization, and application of a lipophilic coated exfoliated Egyptian blue for near-infrared luminescent latent fingermark detection (vol 18, 100208, 2019), FORENSIC Chem. 25 (2021).
[18] V.G. Sears, S.M. Bleay, H.L. Bandey, V.J. Bowman, A methodology for finger mark research, Sci. Justice 52 (3) (2012) 145–160, https://doi.org/10.1016/j.scijus.2011.10.006.
[19] G. Pozza, D. Ajò, G. Chiari, F. De Zuane, M. Favaro, Photoluminescence of the inorganic pigments Egyptian blue, Han blue and Han purple, J. Cult. Herit. 1 (4) (2000) 393–398.
[20] G. Giester, B. Rieck, Effenbergerite, BaCu [Si4O10], a new mineral from the Kalahari Manganese Field, South Africa: description and crystal structure, Mineral. Mag. 58 (393) (1994) 663–670.
[21] E. Kendrick, C.J. Kirk, S.E. Dann, Structure and colour properties in the Egyptian Blue Family, M1−xM′xCuSi4O10, as a function of M, M′ where M, M′=Ca, Sr and Ba, Dyes Pigments 73 (1) (2007) 13–18, https://doi.org/10.1016/j.dyepig.2005.10.006.
[22] P. Mirti, L. Appolonia, A. Casoli, et al., Spectrochemical and structural studies on a roman sample of Egyptian blue, Spectrochim. Acta Part A: Mol. Biomol. Spectrosc. 51 (3) (1995) 437–446, https://doi.org/10.1016/0584-8539(94)E0108-M.
[23] A. Sgamellotti, C. Anselmi, An evergreen blue. Spectroscopic properties of Egyptian blue from pyramids to Raphael, and beyond, Inorg. Chim. Acta 530 (2022) 120699.
[24] M. Weller, M.T. Weller, T. Overton, J. Rourke, F. Armstrong, Inorganic Chemistry, Oxford University Press, USA, 2014.
[25] Y. Chen, Y. Zhang, S. Feng, Hydrothermal synthesis and properties of pigments Chinese purple BaCuSi2O6 and dark blue BaCu2Si2O7, Dyes Pigments 105 (2014) 167–173, https://doi.org/10.1016/j.dyepig.2014.01.017.
[26] M.M. Coimbra, I. Martins, S.M. Bruno, et al., Shedding light on cuprorivaite, the Egyptian Blue pigment: joining neutrons and photons for a computational spectroscopy study, Cryst. Growth Des. (2023).
[27] G. Accorsi, G. Verri, M. Bolognesi, et al., The exceptional near-infrared luminescence properties of cuprorivaite (Egyptian blue), Chem. Commun. (23) (2009) 3392–3394, https://doi.org/10.1039/B902563D.
[28] W. Chen, Y. Shi, Z. Chen, et al., Near-infrared emission and photon energy upconversion of two-dimensional copper silicates, J. Phys. Chem. C. 119 (35) (2015) 20571–20577.
[29] S.M. Borisov, C. Würth, U. Resch-Genger, I. Klimant, New life of ancient pigments: application in high-performance optical sensing materials, Anal. Chem. 85 (19) (2013) 9371–9377, https://doi.org/10.1021/ac402275g.
[30] G. Selvaggio, M. Weitzel, N. Oleksiievets, et al., Photophysical properties and fluorescence lifetime imaging of exfoliated near-infrared fluorescent silicate nanosheets, Nanoscale Adv. 3 (15) (2021) 4541–4553, https://doi.org/10.1039/D1NA00238D.
[31] G. Selvaggio, A. Chizhik, R. Nißler, et al., Exfoliated near infrared fluorescent silicate nanosheets for (bio) photonics, Nat. Commun. 11 (1) (2020) 1495.
[32] J.R. Lakowicz, Principles of Fluorescence Spectroscopy, Springer, 2006.
[33] B. Jones, J. Cammidge, C. Evans, et al., Degradation of polymer banknotes through handling, and effect on fingermark visualisation, Sci. Justice 62 (5) (2022) 644–656.
[34] A. Rafiei, A. Karimi, M. Bodaghi, Polymer banknotes: a review of materials, design, and printing, Sustainability 15 (4) (2023) 3736.

[35] N. Jones, M. Kelly, M. Stoilovic, C. Lennard, C. Roux, The development of latent fingerprints on polymer banknotes, J. Forensic Identif. 53 (1) (2003) 50.
[36] S. Wang, E. Toreini, F. Hao, Anti-counterfeiting for polymer banknotes based on polymer substrate fingerprinting, IEEE Trans. Inf. Forensics Secur. 16 (2021) 2823–2835.
[37] P. Fritz, A. Frick, W. Van Bronswijk, et al., Variability and subjectivity in the grading process for evaluating the performance of latent fingermark detection techniques, J. Forensic Identif. 65 (5) (2015) 851–867.
[38] T. Hanna, S. Chadwick, S. Moret, Fingermark quality assessment, a transversal study of subjective quality scales, Forensic Sci. Int. 350 (2023) 111783.
[39] A.A. Frick, G. Chidlow, S.W. Lewis, W. van Bronswijk, Investigations into the initial composition of latent fingermark lipids by gas chromatography–mass spectrometry, Forensic Sci. Int. 254 (2015) 133–147, https://doi.org/10.1016/j.forsciint.2015.06.032.